GALLOPING ANALYSIS OF A STAY CABLE WITH AN ATTACHED VISCOUS DAMPER CONSIDERING COMPLEX MODES

Cung H. Nguyen[1], John H. G. Macdonald[2]

[1] Ph.D, Lecturer, Department of Civil Engineering, Industrial University of Ho Chi Minh City, 12 Nguyen Van Bao, Go Vap, Ho Chi Minh City, Vietnam. (Corresponding author). Email: nguyenhuycung@iuh.edu.vn

[2] Ph.D, Reader, Department of Civil Engineering, University of Bristol, Queen's Building, University Walk, Bristol BS8 1TR, UK. Email: John.Macdonald@bristol.ac.uk

Abstract

The use of viscous dampers to mitigate cable vibrations on cable-stayed bridges is very popular. A viscous damper attached to a stay cable results in complex mode shapes. Such complexity could affect the dynamic stability of the cable under wind action, yet it is neglected in conventional galloping analysis. A general framework to investigate the problem of galloping of a stay cable with an attached viscous damper is therefore developed. Aerodynamic forces on the complex modes are considered, including aeroelastic coupling between the modes. A numerical example for an ice-accreted stay cable with a damper shows that conventional galloping analysis overestimates the critical wind speed for galloping occurrence. The complexity of the mode shapes gives rise to the cable being more unstable than ignoring it by treating the mode shapes as real.

Keywords: Galloping; Complex mode; Viscous damper; Cable dynamics; Cable-stayed bridges; Quasi-steady theory; Aeroelasticity; Dynamic stability.

Introduction

Stay cables, such as members of cable-stayed bridges, are vulnerable to large vibrations as their inherent damping is very low. A solution widely used in practice to reduce the vibrations is to install a viscous damper transversely to the cable near the cable anchorage. Such a damper is designed to have a damping coefficient that can be optimally tuned for maximum damping ratio of one targeted mode of vibration. Many investigations, e.g. Carne (1981); Krenk (2000); Main and Jones (2002); Pacheco et al. (1993); Uno et al. (1991); Yoneda and Maeda (1989), have been proposed to understand the natural dynamic properties of a cable with an attached viscous damper in free vibration and then to design an optimal damper. Meanwhile, based on the authors' knowledge, its dynamic behaviour under wind action has never been discussed. This is an important issue as cables are very susceptible to wind, and cable-wind interaction is the main cause of the violent vibration of cables which can result in galloping instability (Caetano 2007; Fujino et al. 2012).

In the efforts to find the damping properties of the cable-damper system, the free vibration case has been analysed to solve the eigenvalue problem, in which the cable is usually modelled as a taut string. The first study is credited to Carne (1981). He formulated the complex eigenvalue problem and provided an approximate solution through a numerical procedure. The damping ratio of the first mode was then given. Subsequently, Yoneda and Maeda (1989) and Uno et al. (1991) used a numerical approach to identify the optimal modal damping which depends on the distance between the damper and the cable anchorage. Pacheco et al. (1993) used the Galerkin method to estimate the complex frequencies of the cable-damper system and then introduced a universal curve which links the normalized modal damping ratio of the target mode with the normalized damping coefficient of the attached damper. The universal curve provided a very efficient tool for the design of the damper. This curve was then formulated analytically by Krenk (2000), in which the asymptotic solution for the free vibration of the cable-damper system was derived, using complex modes and assuming that the damper location is near the cable anchorage.

In galloping analysis, the most used method in practice is the Glauert-Den Hartog criterion, in which the structure is prone to galloping in the across-wind direction when the aerodynamic damping is negative (Glauert 1919; Den Hartog 1932). By including the effect of Reynolds number and relative angle between the wind and structure, Macdonald and Larose (2006) generalised the across-wind galloping condition and applied it to inclined cables. Jones (1992) took into account the inherent coupling between along-wind and across-wind vibrations to derive the galloping condition for a two degree-of-freedom (2DOF) system when the two fundamental natural frequencies associated with along-wind and across-wind directions are identical (the resonant condition). More general frameworks to study the coupled galloping phenomena with 3DOF systems have been presented by Piccardo (1993), Yu et al. (1993a), Yu et al. (1993b). Applied to a variety of typical shapes of ice-accreted cables, the study emphasised the importance of the effect of the coupling between along-wind and across-wind effects. Luongo and Piccardo (2005) explained qualitatively the coupled translational galloping phenomenon studied by Jones (1992) with perturbation solutions for the resonant and non-resonant conditions. Carassale et al. (2005) and Macdonald and Larose (2008a) generalised the 2DOF galloping problem for cylinders that have arbitrary attitudes with respect to the wind. In particular, the later provided an analytical formula for the damping necessary to be added to a prismatic structure to prevent the occurrence of galloping in the general condition. Recently, Nguyen et al. (2015) developed a criterion for the coupled translational galloping condition for slender structures with generic cross-sections, taking into account structural eccentricities, modes shapes, higher modes and the variation of mass, width of cross-section and aerodynamic coefficients along the structure, which have not been included in previous studies.

It is important to note that there do not appear to have been any studies addressing galloping analysis that specifically include an attached damper, which results in complex modes. In galloping analysis, the cable is normally modelled on a modal basis with certain modal damping ratios, either as a two-dimensional cross-section problem or using real mode shapes. The Glauert-Den Hartog criterion has been mostly used in practice thanks to its simplicity. Where vibrations in two planes have been consider implicitly, the modes shapes in the cable-damper plane have been treated as the same as those in the other cable plane. Allowing for the aeroelastic coupling between the planes, this results in the 2DOF resonant condition for the occurrence of galloping being independent from the mode shapes for uniform cables in uniform wind (Macdonald and Larose 2008a; Nikitas and Macdonald 2014). However, these approaches may incorrectly predict the galloping condition when there is a discrete damper present as they do not consider the complexity of the mode shapes which is a significant characteristic of a cable-damper system.

This paper aims to formulate the problem of galloping instability of a stay cable with an attached viscous damper in each principal direction, taking into account the complex mode shapes, the aeroelastic forces and possible variations of width of cross-section and aerodynamic coefficients along the structure. First, the equation of motion of a taut cable with an attached damper, subjected to a general external force, is given and a method for calculating the complex modes is presented, which is a variation of previous methods. Then the aeroelastic forces, based on quasi-steady theory, are introduced and the condition for the occurrence of galloping of the coupled system under wind action is established. Finally, an application of the proposed theory to real cases of cables with ice accretion is presented and the effects of the addition of the damper, aeroelastic coupling of modes and the complexity of the mode shapes are discussed.

To avoid confusion, in the rest of the paper the coupling between the two cable planes is referred to as "plane coupling" and the coupling between modes in a single plane is referred to as "modal coupling".

Equation of motion and complex structural modes

Consider an undamped stay cable, neglecting sag, with length L in a Cartesian coordinate system xyz as illustrated in Fig. 1, in which z is along the cable axis while y and x are translational principal axes. In the yz-plane, hereafter simply referred to as the y-plane, as is common, a viscous damper with damping coefficient c is attached to the cable at $z=d$.

The equation of motion of a taut cable with an attached viscous damper is usually formulated by modifying the equation of motion of an undamped taut string with the addition of the damping force and neglecting any inherent damping of the cable. The equation of motion in the cable-damper plane is expressed as (Pacheco et al. 1993):

$$m\ddot{q}(z,t) + \mathrm{D}\dot{q}(z,t) + \mathrm{K}\left[q(z,t)\right] = f(z,t) \tag{1}$$

where m is the mass per unit length, assuming to be constant along the cable; $q(z,t)$ is the displacement; dot stands for time derivative; $\mathrm{K} = -T\partial^2 / \partial z^2$ is a spatially differential stiffness operator; T is the tension force; $f(z,t)$ is the external force; $\mathrm{D} = c\delta(z-d)$, where $\delta(.)$ is the Dirac delta function.

The boundary conditions are given by:

$$q(0,t) = q(L,t) = 0;\ \ \dot{q}(0,t) = \dot{q}(L,t) = 0 \tag{2}$$

$$T\left[q'\left(d^+,t\right) - q'\left(d^-,t\right)\right] = c\dot{q}(d\ \ ,t) \tag{3}$$

where the prime denotes the spatial derivative.

For the system represented by Eq. (1), it is burdensome to derive the mode shapes which satisfy all the conditions given in Eq. (2)-(3). Krenk (2000) and Main and Jones (2002) considered the cable as two separated segments with two cable coordinates, to the left and right of the damper location (Fig. 1), and derived the mode shapes for each cable segment, which can each be treated as an undamped taut string. In their formulations, however, the derivatives of the mode shapes of the whole cable are not continuous functions, so it is not convenient to integrate them over the whole cable when necessary, e.g. for the evaluation of the response of a damper-cable system to external loads (Krenk 2004; Nielsen and Krenk 2003). To overcome this limitation and to avoid using more than one coordinate variable, the mode shape of the whole cable is expressed in a single function as:

$$\phi_n(z) = \phi_n(d)\left\{\psi_n(z,d) + \left[\psi_n(L-z,L-d) - \psi_n(z,d)\right]\mathcal{H}(z-d)\right\} \tag{4}$$

where $\mathcal{H}(z-d)$ is the Heaviside function and $\psi_n(z,d)$ is given by (Krenk 2000):

$$\psi_n(z,d)=\frac{\sin(\beta_n z)}{\sin(\beta_n d)} \tag{5}$$

where n is the mode number; β_n is the n^{th} wave number, related to the n^{th} eigenvalue λ_n of the system governed by Eq. (1) by $\beta_n=-\mathrm{i}\lambda_n\sqrt{m/T}$, being i the imaginary number. At this moment, λ_n is still unknown and will be discussed later.

Then it is possible to differentiate $\phi_n(z)$ at every point along the cable in the classical sense:

$$\begin{aligned}\phi_n'(z)=\phi_n(d)\Big\{&\psi_n'(z,d)-\left[\psi_n'(L-z,L-d)+\psi_n'(z,d)\right]\mathcal{H}(z-d)\\&+\left[\psi_n(L-z,L-d)-\psi_n(z,d)\right]\delta(z-d)\Big\}\end{aligned} \tag{6}$$

$$\begin{aligned}\phi_n''(z)=\phi_n(d)\Big\{&\psi_n''(z,d)+\left[\psi_n''(L-z,L-d)-\psi_n''(z,d)\right]\mathcal{H}(z-d)\\&-2\left[\psi_n'(L-z,L-d)+\psi_n'(z,d)\right]\delta(z-d)+\left[\psi_n(L-z,L-d)-\psi_n(z,d)\right]\delta'(z-d)\Big\}\end{aligned} \tag{7}$$

As a result, it is also possible to integrate terms of $\phi_n'(z)$ and $\phi_n''(z)$ along the whole length of the cable.

To evaluate the response or stability of the cable-damper system, it is necessary to decouple Eq.(1) into single degree-of-freedom (SDOF) systems. Commonly, modal analysis is employed to decouple the equation of motion of a continuous system or a multi degree-of-freedom (MDOF) system into a set of second-order ordinary differential equations of SDOF systems. However, this approach can be applied only for classically damped systems, in which the mode shapes are real and orthogonal with respect to the mass. For a non-classically damped system, the mode shapes are not orthogonal with respect to the mass, so an alternative technique to deal with this issue is required, as introduced in the Appendix. This extends the modal decomposition method for a MDOF system, presented in the standard textbook by Hurty and Rubinstein (1964), to a continuous system. The decoupled equations of motion, in first-order form, instead of second-order form as in classical analysis, are then given by:

$$\dot{p}_n(t) - \lambda_n p_n(t) = \frac{1}{g_n} f_n(t); \quad n = 1,2,3... \tag{8}$$

where $p_n(t)$ are modal coordinates, and

$$g_n = \int_0^L \boldsymbol{\psi}_n^{\mathrm{T}} \begin{bmatrix} 0 & m \\ m & \mathrm{D} \end{bmatrix} \boldsymbol{\psi}_n dz; \quad \boldsymbol{\psi}_n = \begin{bmatrix} \lambda_n \phi_n(z) & \phi_n(z) \end{bmatrix}^{\mathrm{T}} \tag{9}$$

$$f_n(t) = \int_0^L \boldsymbol{\psi}_n^{\mathrm{T}} \mathbf{f} dz; \quad \mathbf{f} = \begin{bmatrix} 0 & f(z,t) \end{bmatrix}^{\mathrm{T}} \tag{10}$$

The eigenvalues λ_n can be expressed in terms of their real and imaginary parts (Igusa et al. 1984; Pacheco et al. 1993; Veletsos and Ventura 1986):

$$\lambda_n = \tilde{\omega}_n \left[-\xi_n + \mathrm{i}\sqrt{1 - \xi_n^2} \right] \tag{11}$$

where $\tilde{\omega}_n = |\lambda_n|$ is the modulus of λ_n; $\xi_n = -\mathrm{Re}[\lambda_n] / |\lambda_n|$ is the modal damping ratio.

The n^{th} eigenvalue of a non-classically damped system given in Eq. (11) is expressed in the same form as that of a classically damped SDOF system with an undamped natural frequency $\tilde{\omega}_n$ and a damping ratio ξ_n. Its real part measures the rate of decay of the modal motion while its imaginary part quantifies the damped natural frequency. As $\tilde{\omega}_n$ here depends on the damping term, it is different from the natural frequency of the undamped system, i.e. the cable without the damper attached, which is $n\pi / \left(L\sqrt{m/T} \right)$. When no damper is attached to the cable, $\tilde{\omega}_n$ is equal to this value of the undamped frequency.

It is worth remembering that the presence of the discrete damper results in complex eigenvalues and modes shapes in conjugate pairs. For an *N*-DOF system, there are *N* pairs of complex eigenvalues and *N* pairs of corresponding modes shapes. The conjugate of Eq.(8) is then given by:

$$\dot{\bar{p}}_n(t) - \bar{\lambda}_n \bar{p}_n(t) = \frac{1}{\bar{g}_n} \bar{f}_n(t); \quad n = 1,2,3... \tag{12}$$

where the overbar denotes the complex conjugate.

Finally, the solutions of Eqs. (8) and (12) can be found when the eigenvalues λ_n are known. Generally, they can be determined numerically starting from the equilibrium condition Eq. (3) (Pacheco et al. 1993). For the special case that the damper is close to the anchorage, i.e. *d*<<*L*, the asymptotic solutions are given by Krenk (2000):

$$\lambda_n = \mathrm{i}\left(n\pi + \frac{\mathrm{i}\eta\kappa_n^2}{1+\mathrm{i}\eta\kappa_n}\right)\frac{1}{L}\sqrt{\frac{T}{m}} \tag{13}$$

where $\eta = c/\sqrt{Tm}$; $\kappa_n = n\pi d/L$.

Inserting Eq. (13) into Eq. (5) and then Eq. (4), the complex mode shapes of a cable with an attached damper close to the anchorage are identified in closed-forms. As an example, for a cable with an attached damper at *d/L*=0.08, Fig. 2 shows the real and imaginary parts of first two mode shapes in the cable-damper plane, i.e. *y*-plane, optimised for the first mode. The mode shapes are normalised such that their values at the damper location are unity. It can be seen that, at the damper location, there is a kink in the mode shape of each mode in the *y*-plane. This is due to the presence of the damper, leading to the discontinuity condition given in Eq. (3). On the other hand, the modes in the *x*-plane (strictly the *xz*-plane), in which no damper is attached, are real and sinusoidal. When the damper location tends to the cable anchorage, the real parts of the mode shapes in the *y*-plane tend to the corresponding mode shapes in the *x*-plane, i.e. they become sinusoidal. The complex mode shapes shown herein agree with those previously presented by Krenk (2004) (but with the damper at a different location along the cable in this example).

Coupled translational galloping analysis

The structural response is a summation of all modal responses, which are grouped in conjugate pairs, e.g. $\phi_n(z)p_n(t)+\bar{\phi}_n(z)\bar{p}_n(t)$. For a system with real mode shapes, it is demonstrated widely in the literature, e.g. in Hurty and Rubinstein (1964), that the imaginary parts of the modal responses cancel out in the total response. Consequently, it is possible to use only the real terms to compute the total response. However, for a system with complex mode shapes, which result in phase differences between modal responses, the imaginary parts of $\phi_n(z)$ and $p_n(t)$ contribute to the total response. This is demonstrated in the Appendix. As a consequence, all conjugate pairs of modal responses are involved in the galloping analysis presented below.

The previous section described the motion of the cable with an attached damper in one plane. However, for coupled translational galloping analysis, which involves motion in both the *x* and *y* planes, it is more general to consider that one damper is attached in each plane. Mathematically, to identify a term related to the *α*-plane (*α*=*x,y*), a subscript *α* is added to that term. For example, c_x and c_y are the damping coefficients in the *x*-plane and *y*-plane, respectively. If there is no damper attached in the *x*-plane, then c_x=0. This notation is used hereon.

The situation is considered where the external load is an aeroelastic load resulting from the interaction between the wind and the structure. In this study, the wind is taken to be normal to the cable axis. Based on the quasi-steady assumption, this load is expressed in terms of the structural velocity. Then, ignoring any nonlinear and torsional terms and assuming that there are in total *N* modes in the *α*-plane (*α*=*x,y*) contributing to the structural response, the n^{th} modal loads for wind normal to the cable axis are given by:

$$\begin{gathered}
\begin{Bmatrix} f_{n,x}(t) \\ f_{n,y}(t) \end{Bmatrix} = -\frac{1}{2}\rho\int_0^L U(z)b(z)\begin{bmatrix} \phi_{n,x}(z) & 0 \\ 0 & \phi_{n,y}(z) \end{bmatrix}\mathbf{C}_a\mathbf{\Psi}\dot{\mathbf{P}}dz \\
\begin{Bmatrix} \bar{f}_{n,x}(t) \\ \bar{f}_{n,y}(t) \end{Bmatrix} = -\frac{1}{2}\rho\int_0^L U(z)b(z)\begin{bmatrix} \bar{\phi}_{n,x}(z) & 0 \\ 0 & \bar{\phi}_{n,y}(z) \end{bmatrix}\mathbf{C}_a\mathbf{\Psi}\dot{\mathbf{P}}dz
\end{gathered} \tag{14}$$

where ρ, $U(z)$ and $b(z)$ are the density of air, mean wind velocity and reference width of the cross-section of the cable, respectively, and

$$\mathbf{\Psi} = \begin{bmatrix} \mathbf{\Psi}_x & \mathbf{O}_{2N} \\ \mathbf{O}_{2N} & \mathbf{\Psi}_y \end{bmatrix} \tag{15}$$

$$\mathbf{O}_N = \begin{bmatrix} 0 & 0 \ldots 0 \end{bmatrix}_{1\times N} \tag{16}$$

$$\mathbf{\Psi}_\alpha = \begin{bmatrix} \mathbf{\Phi}_\alpha & \bar{\mathbf{\Phi}}_\alpha \end{bmatrix} \tag{17}$$

$$\mathbf{\Phi}_\alpha = \begin{bmatrix} \phi_{1,\alpha}(z) & \phi_{2,\alpha}(z) & \ldots & \phi_{\mathrm{N},\alpha}(z) \end{bmatrix} \tag{18}$$

$$\mathbf{P} = \begin{bmatrix} \mathbf{P}_x & \bar{\mathbf{P}}_x & \mathbf{P}_y & \bar{\mathbf{P}}_y \end{bmatrix}^{\mathrm{T}} \tag{19}$$

$$\mathbf{P}_\alpha = \begin{bmatrix} p_{1,\alpha}(t) & p_{2,\alpha}(t) & \ldots & p_{N,\alpha}(t) \end{bmatrix} \tag{20}$$

$$\mathbf{C}_a = \mathbf{R}^{\mathrm{T}}\mathbf{C}_{a0}\mathbf{R} \tag{21}$$

$$\mathbf{R} = \begin{bmatrix} \cos\gamma & \sin\gamma \\ -\sin\gamma & \cos\gamma \end{bmatrix} \tag{22}$$

$$\mathbf{C}_{a0} = \begin{bmatrix} 2C_d(z,\theta) & C_d'(z,\theta) - C_l(z,\theta) \\ 2C_l(z,\theta) & C_d(z,\theta) + C_l'(z,\theta) \end{bmatrix} \tag{23}$$

in which γ is the angle between the wind and the axis *x*; C_d and C_l are the drag and lift coefficients; C_d' and C_l' are their derivatives with respect to the angle of attack θ, i.e. the angle between the wind and a reference line on the cross-section.

In general, the aerodynamic coefficient matrix $\mathbf{C}_{a0}$ is full. Therefore the modal aeroelastic loads given in Eq.(14) involve the plane coupling.

To formulate the galloping analysis problem, Eq. (14) is substituted into Eqs. (8) and (12), and the obtained equations can arranged in following matrix form:

$$\mathbf{AP} + \mathbf{B}\dot{\mathbf{P}} = \mathbf{0} \tag{24}$$

where

$$\mathbf{A} = \mathrm{diag}\left[\mathbf{A}_x \quad \bar{\mathbf{A}}_x \quad \mathbf{A}_y \quad \bar{\mathbf{A}}_y\right] \tag{25}$$

$$\mathbf{A}_\alpha = -\left[\lambda_{1,\alpha} g_{1,\alpha} \quad \lambda_{2,\alpha} g_{2,\alpha} \quad \cdots \quad \lambda_{N,\alpha} g_{N,\alpha}\right] \tag{26}$$

$$\mathbf{B} = \mathbf{G} + \tilde{\mathbf{C}}_a \tag{27}$$

$$\mathbf{G} = \mathrm{diag}\left[\mathbf{G}_x \quad \bar{\mathbf{G}}_x \quad \mathbf{G}_y \quad \bar{\mathbf{G}}_y\right] \tag{28}$$

$$\mathbf{G}_\alpha = \mathrm{diag}\left[g_{1,\alpha} \quad g_{2,\alpha} \quad \cdots \quad g_{N,\alpha}\right] \tag{29}$$

$$\tilde{\mathbf{C}}_a = \frac{1}{2}\rho\int_0^L U(z)\,b(z)\,\mathbf{\Psi}^{\mathrm{T}}\mathbf{C}_a\mathbf{\Psi}\,dz \tag{30}$$

Galloping occurs, i.e. the system is unstable, if there exists an eigenvalue of Eq.(24), denoted Λ, such that its real part, Re(Λ), is positive. The mean wind velocity at which Re(Λ) is zero is referred to as the critical wind velocity. The meaning of the critical wind velocity is that when it is lower than the mean wind velocity, the structure will gallop. Conventionally, the critical velocity is a constant value. However, for non-horizontal structures, the variation of mean wind velocity along the structure, governed by the mean wind profile, contributes to the eigenvalues of Eq. (24). It is therefore necessary to use a critical wind profile, which was first introduced in Nguyen et al. (2015), as:

$$U_{cr}(z) = U_{cr}(z_e)\,\mu(z) \tag{31}$$

where z_e is a suitable reference height (not chosen in close proximity to the ground); $U_{cr}(z_e)$ is the critical wind velocity at z_e, and $\mu(z)$ is a non-dimensional function expressing the shape of the mean wind velocity profile, e.g. a power or logarithmic law.

It is worth noting that for a uniform structure in uniform wind with the same mode shapes in each plane, the structural stability is unaffected by the modes shapes (Macdonald and Larose 2008a; Nikitas and Macdonald 2014). However, if the cable has a damper attached in one plane, the mode shapes in the two planes are different. They then play a role in the structural stability even when theaerodynamic coefficients and wind velocity are constant. The reason comes from the fact that the modes shapes are no longer orthogonal to each other (see the Appendix), so the relevant cross-terms in Eq. (24) are non-zero.

It can be said that Eq.(24) governs the general problem of linear galloping instability of line-like structures, in which variation of the aerodynamic coefficients and mean wind velocity along the structure, the presence of dampers and the role of complex modes shapes are all taken into account. Its eigenvalues, which give conditions for the occurrence of galloping, can be therefore considered as rigorous solutions. As the full problem has not previously been addressed in the literature, it is useful to link the rigorous analysis with simplified ones, without the attached damper and/or without the plane coupling. For this purpose, two main cases are considered:

Case 1: *with damper.* Only one damper is attached to the cable, in the *y*-plane. The mode shapes in the *x*-plane are hence real. Then the structural stability analysis can be conducted by solving the eigenvalue problem of Eq. (24) with the elimination of the following terms:

(1.i). $\bar{\mathbf{A}}_x$, $\bar{\mathbf{G}}_x$ and $\bar{\mathbf{\Phi}}_x$ if the plane coupling is considered.

(1.ii). $\mathbf{A}_x$, $\bar{\mathbf{A}}_x$, $\mathbf{G}_x$, $\bar{\mathbf{G}}_x$, $\mathbf{\Phi}_x$ and $\bar{\mathbf{\Phi}}_x$ if the plane coupling is neglected.

The sub-cases (1.i) and (1.ii) are referred to as "*xy* coupled (with damper)" and "*y* uncoupled (with damper)", respectively. It should be noted that the modal coupling in the *y*-plane is always considered in these cases.

Case 2: without (w/o) damper. The case is considered when no damper is attached to the cable. So the natural frequencies as well as the mode shapes in the two cable planes are identical, which is true for a taut string. Following sub-cases can occur, varying from complex to simple cases:

(2.i). Modal coupling and plane coupling are considered. Then the stability analysis can be conducted by solving the eigenvalue problem of Eq. (24) with the elimination of the conjugate terms, i.e. $\bar{\mathbf{A}}_x$, $\bar{\mathbf{A}}_y$, $\bar{\mathbf{G}}_x$, $\bar{\mathbf{G}}_y$, $\bar{\mathbf{\Phi}}_x$ and $\bar{\mathbf{\Phi}}_y$.

(2.ii). Plane coupling is considered and modal coupling are negligible. This sub-case is referred to as "*xy* coupled (w/o damper)." The case falls into the 2DOF model of coupled translational galloping, in which the condition for the occurrence of galloping in the k^{th} x-plane and the k^{th} y-plane modes is given by (Nguyen et al. 2015):

$$C_{a,xy,k,eq} < 0 \tag{32}$$

where

$$C_{a,xy,k,eq} = \mathrm{Re}\left[\mathrm{tr}\mathbf{C}_{a,xy,k,eq} - \sqrt{\mathrm{tr}^2\mathbf{C}_{a,xy,k,eq} - 4\det\mathbf{C}_{a,xy,k,eq}}\right] \tag{33}$$

$$\mathbf{C}_{a,xy,k,eq} = \frac{1}{2}\rho U\left(z_e\right)\int_0^L \mu\left(z\right) b\left(z\right) \mathbf{\Psi}_k^{\mathrm{T}} \mathbf{C}_{a0} \mathbf{\Psi}_k dz \tag{34}$$

$$\mathbf{\Psi}_k\left(z\right) = \begin{bmatrix} \phi_{k,x} & 0 \\ 0 & \phi_{k,y} \end{bmatrix} \tag{35}$$

in which tr(.) and det(.) stand for the trace and determinant of a matrix, respectively.

If the aerodynamic coefficients are constant along the structure, the conditions in Eq. (32) drastically simplify to the following closed form (Nguyen et al. 2015):

$$C_{a,xy} < 0 \tag{36}$$

where

$$C_{a,xy} = \mathrm{Re}\left[\mathrm{tr}\left(\mathbf{C}_{a0}\right) - \sqrt{\mathrm{tr}^2\left(\mathbf{C}_{a0}\right) - 4\det\left(\mathbf{C}_{a0}\right)}\right] \tag{37}$$

The aerodynamic damping term given by Eq. (37), along with the condition in Eq. (36), agrees with the equivalent conditions derived for 2DOF coupled translational galloping of a uniform structures in uniform wind by Jones (1992) and Macdonald and Larose (2008a), but here Eqs.(33)-(35), along with the condition in Eq.(32), are still applicable for non-uniform structures in non-uniform wind.

(2.iii). Plane coupling and modal coupling are neglected. It is common to consider across-wind galloping of a single mode, in which the wind is along the x-direction, and the along-wind vibrations are ignored. This sub-case is referred to as "*y* uncoupled (w/o damper)." This case is relevant when the along-wind and across-wind modes are well separated (Luongo and Piccardo 2005; Macdonald and Larose 2008b; Nikitas and Macdonald 2014). Then the conditions in Eq.(32) and Eq. (36) are reduced to (Nguyen et al. 2015):

$$C_{a,y,k,eq} < 0 \tag{38}$$

where

$$C_{a,y,k,eq} = \frac{1}{2}\rho U\left(z_e\right)\int_0^L \mu\left(z\right)b\left(z\right)\left[C_d\left(z\right)+C_l'\left(z\right)\right]\phi_{k,y}^2\left(z\right)dz \tag{39}$$

If the aerodynamic coefficients are constant along the structure, the condition in Eq. (38) turns to the well-known Glauert-Den Hartog condition for 1DOF across-wind galloping:

$$C_d + C_l' < 0 \tag{40}$$

It should be noted that conventional galloping analysis, for a single across-wind mode or identical coupled modes in the two planes, addresses the critical cases of galloping occurrence in the first mode in each plane. This is correct if the aerodynamic coefficients are constant, and then the conditions for galloping occurrence are given by Eqs. (36) and (40). However, when the aerodynamic coefficients vary along the structure, it is possible that the conditions given in Eqs. (32) and (38) are not satisfied for the first mode but are satisfied for higher modes. In this case, the structure is stable in the first mode but unstable in higher modes.

The analytical framework described above provides a procedure to conduct galloping analysis in the complex field. If the damper is very close to the cable anchorage, it may result in weak complexity in the structural motion. Then the added damping could be considered as a perturbation of the undamped cable, and the problem could be addressed with another approach such as perturbation analysis (Luongo et al. 2008; Luongo and Zulli 2014). However, the proposed method is more general and exact so is applicable for any damper location or other parameter values, in which case the complexity may not be so weak.

Application

As an example, a taut bridge cable with an attached viscous damper in the y-plane (vertical plane) is considered, as in Pacheco et al. (1993), in which the parameters are L=215.11 m, b=0.2 m, d/L=0.08, T=3.69x10^6 N, m=98.6 kg/m. To focus on studying the effect of the attached damper, the cable is considered as an undamped one when no damper device is attached. The cable is assumed to be inclined at 20^o with respect to the horizontal plane. The bridge is located in terrain characterized by a roughness length z_0 = 0.3 m. The wind direction is taken to be in the x-direction, i.e. normal to the cable axis and γ=0°. It is assumed that the mean wind velocity profile follows the logarithmic rule and the turbulence has negligible effect on the aerodynamic coefficients of the cable. The reference height is z_e = 10 m above the ground. The non-dimensional function for mean wind profile is given by:

$$\mu\left(z\right)=\frac{\ln\left(z/z_0\right)}{\ln\left(z_e/z_0\right)} \tag{41}$$

As the damper is near the cable anchorage, the natural frequencies of the damper-cable system can be taken as in Eq. (13). In addition, assuming that the damper is optimised for the first mode of cable vibration, the optimised damping ratio for that mode is approximately (Krenk 2000; Main and Jones 2002):

$$\xi_{opt}=\frac{d}{2L} \tag{42}$$

In the presence of the damper, the modes in the y-plane are complex. First two mode shapes in the y-plane are already shown in Fig. 2.

To investigate the galloping behaviour when the damper is attached to the cable, the aerodynamic coefficients for an ice-accreted cable are taken from wind tunnel tests by Gjelstrup et al. (2012). The examined coefficients are C_d=0.95, C_l=0.23, C'_d=1.77, C'_l=-2.43, for angle of attack -30° associated with reference axes system defined in Gjelstrup et al. (2012) but they can be considered for the angle of attack θ=0° in this paper just by rotating the reference axes. The mass of the ice is assumed to be negligible relative to the mass of the cable.

In the galloping analysis, 10 structural modes in each plane are considered. The plane coupling and modal coupling are taken into account.

Fig. 3 shows the real parts of the first 20 eigenvalues corresponding to the first 20 modes of the coupled system versus the mean wind velocity at the reference height z_e. The lighter lines correspond to the higher system modes. Here the term "system modes" refers to modes of the whole system of the structure and the wind, and it is distinguished from the structural modes, which depend only on the structure itself and are independent of the wind. Based on the eigenvalues, the stability condition of different modes can be determined.

Two important points can be realised. Firstly, for the odd system modes, which essentially correspond to along-wind vibrations, the real parts of the eigenvalues are always negative, i.e. they are stable. Meanwhile, for the even system modes, which correspond to predominantly across-wind vibrations, the real parts of the eigenvalues become positive for $U(z_e) \geq 70$ m/s. Secondly, the system is more unstable in lower system modes. These observations imply that the stability of the system can be evaluated through only the lowest predominantly across-wind system mode.

The eigenvalues shown in Fig. 3 are rigorous solutions, allowing for complex modes due to the presence of the damper and the modal coupling in each plane. As mentioned in the previous section, to identify the significance of different effects, it is useful to compare the results with those obtained from simplified analyses, without the damper and/or without the plane coupling. For this purpose, four cases (1.i), (1.ii), (2.ii) and (2.iii), described in the previous section, are considered. Case (2.i) is not included here because it falls into case (2.ii), resulting from the reason stated above that the stability of the system can be evaluated through only the first system mode in each plane.

Fig. 3 shows the stability of all 20 system modes included in the analysis, but since a structural system is unstable if there is at least one eigenvalue with a positive real part, using only the maximum value of the real parts of the eigenvalues determines the stability of the system. Therefore, to compare the four cases mentioned above, Fig. 4 shows the maximum values of the real parts of the eigenvalues of the system, for each case, versus the mean wind velocity at the reference height.

Looking at the simplest case of the undamped cable where the vibrations in the two planes are uncoupled, i.e. case (2.iii), it can be seen that the maximum real parts of the eigenvalues (dashed line) are positive, implying that the structural system is unstable. This is because $C_{a,y} = C_d + C_l' = -1.48 < 0$ (Eq. (40)). If the plane coupling is taken into account (2DOF perfectly tuned system), i.e. case (2.ii), the maximum real parts of the eigenvalues (dotted line) are more positive. This shows that the plane coupling makes the structure more unstable than neglecting it. In other words, neglecting such a coupling can overestimate the stability of the structure.

It is worth noting that the eigenvalue lines in the figure mentioned above (i.e. case 2.ii and 2.iii) pass through the origin and do not provide any critical velocity. This is because, with the assumption of an undamped cable, the real parts of all the eigenvalues are simply proportional to the wind speed, so they pass through the origin (i.e. they are neutrally stable for no wind), and the gradient indicates the stability in relation to the wind speed (Luongo and Piccardo 2005; Macdonald and Larose 2006). Adding damping brings the each line down and gives a critical wind speed where it crosses the horizontal axis and which is proportional to the added damping ratio.

When the damper is installed, the stability of the structure is clearly improved. If the plane coupling is neglected, i.e. case (1.ii), for the chosen values, the structural system is still stable for wind velocities up to 80 m/s (cross line). However, the situation changes if the plane coupling is considered (case (1.i)). In this case, the maximum real parts of the eigenvalues (continuous bold line) are positive, i.e. the structure is potentially unstable, for $U(z_e) \geq 70$ m/s as already seen Fig. 3. So, disregarding the plane coupling can considerably overestimate the critical velocity for the occurrence of galloping. This observation highlights the importance of the plane coupling. Neglecting it can give rise to results unsafe to the structure.

As mentioned in the introduction, the complexity of the mode shapes has not been considered in previous galloping analyses. Instead, the mode shapes in the y-plane (cable-damper plane) have implicitly been treated as real by considering them the same as the mode shapes in the orthogonal plane, where there is no attached damper. Rigorously, this approach is incorrect as the mode shapes in the two cable planes are different when a damper is attached to the cable, so then they affect the galloping condition as shown in Eqs. (32)-(40). This means that the complex mode shapes affect the stability of the system.

To understand the role of the complex mode shapes, galloping analysis of the cable-damper system herein is conducted with and without considering the complexity of the y-plane mode shapes $\phi_y(z)$. The analysis comprises 4 cases:

(1.i) The vibrations in the x-plane and y-plane are coupled, and $\phi_y(z)$ are treated as complex. As being investigating the role of complex mode shape, this rigorous case is renamed *"xy* coupled (ϕ_y complex)".

(1.i.r) The two planes are coupled, and $\phi_y(z)$ are treated as the same as $\phi_x(z)$, i.e. $\phi_y(z)$ are real. This case, named *"xy* coupled (ϕ_y real)", is a simplification of the case (1.i).

(1.ii.) The two planes are uncoupled, and $\phi_y(z)$ are treated as complex. For the same reason for the case (1.i) above, this case is renamed *"y* uncoupled (ϕ_y complex)".

(1.ii.r) The two planes are uncoupled, and $\phi_y(z)$ are treated as the same as $\phi_x(z)$. This case, named *"y* uncoupled (ϕ_y real)", is a simplification of the case (1.ii).

It should be noted that in all four cases, the damping of the modes in the y-plane is taken as that in the presence of the damper. Strictly, the real mode shapes are not compatible with this but, this is effectively what has been done in previous galloping analysis in which the damping effect of the damper has been considered but the complexity of the mode shapes has been neglected.

Fig. 5 plots the maximum real part of the eigenvalues of these four cases, versus the mean wind velocity at the reference height. It can be seen as before that, when the y-plane mode shapes $\phi_y(z)$ are treated as complex, the real parts of the eigenvalues are positive, i.e. the system is unstable, for $U(z_e) \geq 70$ m/s and for $U(z_e) \geq 80$ m/s with the plane coupling (continuous line) and without the plane coupling (cross line), respectively. These results have already been shown in Fig. 4 and discussed above. For real $\phi_y(z)$, i.e. $\phi_y(z) = \phi_x(z)$, the critical velocities increase up to 73 m/s with the plane coupling (dash line) and 85 m/s without the plane coupling (dotted line). This indicates the role of the complexity of the mode shapes. Ignoring it can overestimate the critical velocity for the occurrence of galloping, which is unsafe for the structure.

In the above examples, only one set of aerodynamic parameters has been used, but the analysis demonstrates the role of the attached damper, the complex modes and the plane coupling in affecting the stability of the cable-damper system in the wind. For other aerodynamic coefficients, e.g. from Richardson (1988) or Gjelstrup et al. (2012), the behaviour has been found to be qualitatively the same when identifying the effect of the complex modes as shown in the Fig.5. In all cases of negative $C_d + C_l'$, the critical wind speeds are reduced when considering the complex modes. The specific gradients and critical wind velocities vary depending on the parameters. The example shown has demonstrated that the effects can be significant and the same method can be applied to any other specific case to obtain the relevant results. Consequently, it is unsafe to ignore the complexity of the modes.

In the meanwhile, the plane coupling may be beneficial or detrimental to the structural stability depending on the aerodynamic coefficients. For example, for C_d=0.99, C_l=0.13, C'_d=-0.96, C'_l=-1.26 (Gjelstrup et al. 2012), the plane coupling is beneficial as the critical velocity for the coupled 2DOF galloping is higher than that for 1DOF galloping. In contrast, for C_d=1.07, C_l=0.6, C'_d=1.06, C'_l=-1.39 (Richardson 1988), the plane coupling is beneficial as the critical velocity for the coupled 2DOF galloping is higher than that for 1DOF galloping. The role of plane coupling on aeroelastic stability of cables has previously been reported in the literature, e.g. in Luongo and Piccardo (2005); Macdonald and Larose (2008b).

Conclusions

Viscous dampers have been used widely on cable-stayed bridges to dampen cable oscillations. Complexity of the mode shapes and natural frequencies is a particular characteristic of the cable-damper system. A number of studies have been made on this system mainly to find the optimal damping ratio for the purposes of damper design. Meanwhile, previous literature on cable galloping ignored the complexity of the mode shapes. This approach, however, is not accurate as the modal interactions are affected by the complexity of the mode shapes. Rigorous analysis of the galloping of a cable-damper system has not previously been conducted.

To address this omission, this paper has developed a general framework to study the problem of galloping instability of a stay cable with two orthogonal attached viscous dampers, one in each principal cable plane. To be as general as possible, the complex mode shapes, the modal coupling, the plane coupling and variations of the width of cross-section, mean wind velocity and aerodynamic coefficients along the cable are all taken into account. The analysis for the particular case that only one damper is attached to the cable is obtained by setting the damping coefficient associated with the undamped cable plane as zero.

Based on aerodynamic data from the literature, obtained from wind tunnel tests of a stay cable accreted with ice, numerical application of the proposed theory reveals several crucial points of engineering significance. Firstly, the stability analysis can be conducted based on only the first system mode predominantly in the across-wind plane since it is the most critical mode. Secondly, the plane coupling is particularly important. It is shown that the plane coupling may cause critical wind velocities considerably lower than if the plane coupling is ignored. Finally, allowing for the complexity of the mode shapes may cause the cable to be more unstable than if it is ignored, as in common analyses.

All the analyses carried out in this paper are based on assumptions that the sag, bending stiffness and nonlinearity of the cable are negligible. As a preliminary step, this choice is justified by the desire of checking the potential occurrence of critical situations that are unpredictable by means of conventional engineering models. Since the results illustrated in this paper confirm such critical situations, other features could now be included in the analysis such as those mentioned above or other types of dampers. These features may change the dynamic behaviour of the cable subjected to the wind. Galloping analysis in these instances therefore deserves further investigations. For the onset of galloping, nonlinear effects can be linearised about the equilibrium condition. Other structural effects will affect the structural modes but the general framework and the coupled translational galloping analysis presented are still valid.

Acknowledgements

The authors gratefully acknowledge the support of the research by the Newton Fund under the UK Royal Academy of Engineering Newton Research Collaboration Programme, grant number NRCP/1415/292.

The first author is grateful to the Industrial University of Ho Chi Minh City for supporting this research.

Appendix: Motion of a damped system

Homogeneous solutions of Eq. (1) have the following form:

$$q(z,t)=\phi(z)e^{\lambda t} \tag{A.1}$$

Substituting Eq. (A.1) into Eq. (1), the eigenvalue problem is obtained:

$$\lambda^2 m\phi(z)+\lambda \mathrm{D}\phi(z)+\mathrm{K}\phi(z)=0 \tag{A.2}$$

Eq. (A.2) gives an infinite number of solutions for the eigenvalues λ_k $(k=1,2,...)$ and associated eigenvectors $\phi_k(z)$.

Let $\boldsymbol{\psi}_k=\left[\lambda_k\phi_k(z) \quad \phi_k(z)\right]^{\mathrm{T}}$. Then $(\lambda_k,\boldsymbol{\psi}_k)$ and $(\lambda_j,\boldsymbol{\psi}_j^{\mathrm{T}})$ are respectively the right and left homogeneous eigensolutions of the following state space system derived from Eq.(1):

$$\boldsymbol{\Gamma}\dot{\mathbf{Q}}(z,t)+\mathbf{H}\mathbf{Q}(z,t)=\mathbf{f}(z,t) \tag{A.3}$$

where

$$\boldsymbol{\Gamma}=\begin{bmatrix}0 & m\\ m & \mathrm{D}\end{bmatrix};\ \mathbf{H}=\begin{bmatrix}-m & 0\\ 0 & \mathrm{K}\end{bmatrix};\ \mathbf{Q}=\begin{Bmatrix}\dot{q}(z,t)\\ q(z,t)\end{Bmatrix};\ \mathbf{f}(z,t)=\begin{Bmatrix}0\\ f(z,t)\end{Bmatrix}$$

Consequently, the following relationships are established:

$$\lambda_k \boldsymbol{\Gamma}\boldsymbol{\psi}_k + \mathbf{H}\boldsymbol{\psi}_k = \mathbf{0} \tag{A.4}$$

and
$$\lambda_j \boldsymbol{\Gamma}^{\mathrm{T}}\boldsymbol{\psi}_j + \mathbf{H}^{\mathrm{T}}\boldsymbol{\psi}_j = \mathbf{0} \tag{A.5}$$

Pre-multiplying both sides of Eq. (A.4) and Eq. (A.5) by $\boldsymbol{\psi}_j^{\mathrm{T}}$ and $\boldsymbol{\psi}_k^{\mathrm{T}}$, respectively, and then integrating the obtained equations over the domain [0 L], yields:

$$\int_0^L \lambda_k \boldsymbol{\psi}_j^{\mathrm{T}}\boldsymbol{\Gamma}\boldsymbol{\psi}_k dz + \int_0^L \boldsymbol{\psi}_j^{\mathrm{T}}\mathbf{H}\boldsymbol{\psi}_k dz = 0 \tag{A.6}$$

$$\int_0^L \lambda_j \boldsymbol{\psi}_j^{\mathrm{T}}\boldsymbol{\Gamma}\boldsymbol{\psi}_k dz + \int_0^L \boldsymbol{\psi}_j^{\mathrm{T}}\mathbf{H}\boldsymbol{\psi}_k dz = 0 \tag{A.7}$$

Subtracting Eq. (A.7) from Eq. (A.8), the bi-orthogonality of the eigenvectors is obtained:

$$\int_0^L \boldsymbol{\psi}_j^{\mathrm{T}}\boldsymbol{\Gamma}\boldsymbol{\psi}_k dz = g_k \delta_{jk} \tag{A.8}$$

and
$$\int_0^L \boldsymbol{\psi}_j^{\mathrm{T}}\boldsymbol{\Gamma}\boldsymbol{\psi}_k dz = h_k \delta_{jk} \tag{A.9}$$

where δ_{jk} is the Kronecker delta function; g_k and h_k are constants and complex in general.

From Eq.(A.2), (A.8) and (A.9), it is possible to show that:

$$\lambda_k g_k + h_k = 0 \tag{A.10}$$

It should be noted from Eq. (A.8) that if the damping is not proportional to the mass, it gives:

$$\int_0^L m\left(\lambda_j + \lambda_k\right)\phi_j(z)\phi_k(z)\,dz \neq 0 \qquad \text{for } j \neq k \tag{A.11}$$

This means that the mode shapes $\phi_k(z)$ are not orthogonal with each other. For the case of proportional damping, the classical orthogonality of mode shapes is valid.

As all the eigenvectors $\boldsymbol{\psi}_k$ are linearly independent, there exists a set of functions $p_k(t)$, $k = 1, 2, \ldots$ such that:

$$\mathbf{Q}(z,t) = \sum_{j=1}^{\infty} \boldsymbol{\psi}_j p_j(t) \tag{A.12}$$

where $p_j(t)$ is referred to as the modal coordinate.

Inserting Eq. (A.12) into Eq. (A.3), then pre-multiplying both sides of the obtained equation by $\boldsymbol{\psi}_k^{\mathrm{T}}$ and integrating it over the domain [0 L], it results in:

$$\int_0^L \sum_{k=1}^{\infty} \boldsymbol{\psi}_j^{\mathrm{T}} \boldsymbol{\Gamma} \boldsymbol{\psi}_k \dot{p}_k(t) dz + \int_0^L \sum_{k=1}^{\infty} \boldsymbol{\psi}_j^{\mathrm{T}} \mathbf{H} \boldsymbol{\psi}_k p_k(t)\, dz = \int_0^L \boldsymbol{\psi}_j^{\mathrm{T}} \mathbf{f} dz \tag{A.13}$$

Applying the bi-orthogonality in Eq. (A.8-A.9) and the relationship in Eq. (A.10), the equation of motion Eq. (1) can be decoupled into a series of the first order differential equations for SDOF systems:

$$\dot{p}_k(t) - \lambda_k p_k(t) = \frac{1}{g_k} f_k(t) \tag{A.14}$$

where $f_k(t) = \int_0^L \boldsymbol{\psi}_k^{\mathrm{T}} \mathbf{f} dz$ is the modal force.

Similar, but not the same, derivations of decoupled equations of motion for non-proportional damped systems as in Eq. (A.14) can be found widely in the literature, e.g. in the standard textbook Hurty and Rubinstein (1964), which treated for MDOF systems and for symmetric matrices $\boldsymbol{\Gamma}$ and $\mathbf{H}$ containing self-adjoint operators. The derivation described above extends to a continuous system. In addition, by employing a fundamental technique in linear algebra with the left and right eigenvectors of the homogeneous system of Eq. (A.3), it does not require any condition for either the symmetry of the related matrices or adjointability of the operators. So the derivation herein is also valid for general asymmetric matrices with non-self-adjoint operators.

Now, following is a proposed demonstration of how imaginary parts of complex mode shapes and modal coordinates contribute to the response.

The modal response related to mode *n* is given by:

$$q_n(z,t) = \phi_n(z)\, p_n(t) + \bar{\phi}_n(z)\, \bar{p}_n(t) \tag{A.15}$$

As $\phi_{n,\alpha}(z)$ and $p_n(t)$ are complex, they can be expressed in terms of real and imaginary parts as:

$$\phi_n(z) = \phi_{n\mathrm{R}}(z) + \mathrm{i}\phi_{n\mathrm{I}}(z) \tag{A. 16}$$

$$p_n(t) = p_{n\mathrm{R}}(t) + \mathrm{i}p_{n\mathrm{I}}(t) \tag{A. 17}$$

where $\phi_{n\mathrm{R}}(z)$, $\phi_{n\mathrm{I}}(z)$, $p_{n\mathrm{R}}(t)$ and $p_{n\mathrm{I}}(t)$ are real functions, in which the subscripts "R" and "I" stand for "Real" and "Imaginary" parts.

Inserting Eqs. (A.16) and (A.17) into Eq. (A.15), yields:

$$q_n(z,t) = 2\left[\phi_{n\mathrm{R}}(z)\, p_{n\mathrm{R}}(t) - \phi_{n\mathrm{I}}(z)\, p_{n\mathrm{I}}(t)\right] \tag{A. 18}$$

It can be realised that the second term on the right hand side of Eq. (A.18) appears due to the complexity of $\phi_{n,\alpha}(z)$ and $p_n(t)$. Their imaginary parts contribute to the modal responses, hence to the total response of the structure. If the mode shapes are real, the total response can be computed based on only the real parts.

References

Caetano, E. D. S. (2007). *Cable Vibrations in Cable-stayed Bridges*. IABSE (International Association for Bridge and Structural Engineering: www.iabse.org), CH-8093 Zurich, Switzerland.

Carassale, L., Freda, A., and Piccardo, G. (2005). "Aeroelastic forces on yawed circular cylinders: Quasi-steady modeling and aerodynamic instability." *Wind and Structures, An International Journal*, 8(5), 373–388.

Carne, T. G. (1981). "Guy Cable Design and Damping for Vertical Axis Wind Turbines." *Report no. SAND80-2669, Sandia National Laboratory, Albuquerque, N.M*, (SAND80-2669).

Den Hartog, J. P. (1932). “Transmission line vibration due to sleet.” *Transactions of the American Institute of Electrical Engineers*, 51, 1074–1076.

Fujino, Y., Kimura, K., and Tanaka, H. (2012). *Wind resistant design of bridges in Japan*. Springer Japan.

Gjelstrup, H., Georgakis, C. T., and Larsen, A. (2012). “An evaluation of iced bridge hanger vibrations through wind tunnel testing and quasi-steady theory.” *Wind and Structures, An International Journal*, 15(5), 385–407.

Glauert, B. H. (1919). “The rotation of an aerofoil about a fixed axis.” *Report and memoranda, No. 595, British Advisory Committee for Aeronautics (ARC)*, (R & M No. 595), 443–447.

Hurty, W., and Rubinstein, M. . (1964). *Dynamics of Structures*. Prentice-Hall, New Jersey.

Igusa, T., Kiureghian, A. Der, and Sackman, J. L. (1984). “Modal decomposition method for stationary response of non-classically damped systems.” *Earthquake Engineering and Structural Dynamics*, 12(1), 121–136.

Jones, K. F. (1992). “Coupled Vertical and Horizontal Galloping.” *Journal of Engineering Mechanics*, 118(1), 92–107.

Krenk, S. (2000). “Vibrations of a Taut Cable With an External Damper.” *ASME Journal of Applied Mechanics*, 67(4), 772–776.

Krenk, S. (2004). “Complex modes and frequencies in damped structural vibrations.” *Journal of Sound and Vibration*, 270(4–5), 981–996.

Luongo, A., and Piccardo, G. (2005). “Linear instability mechanisms for coupled translational galloping.” *Journal of Sound and Vibration*, 288(4–5), 1027–1047.

Luongo, A., and Zulli, D. (2014). “Aeroelastic instability analysis of NES-controlled systems via a mixed multiple scale/harmonic balance method.” *Journal of Vibration and Control*, 20(13), 1985–1998.

Luongo, A., Zulli, D., and Piccardo, G. (2008). “Analytical and numerical approaches to nonlinear galloping of internally resonant suspended cables.” *Journal of Sound and Vibration*, 315(3), 375–393.

Macdonald, J. H. G., and Larose, G. L. (2006). "A unified approach to aerodynamic damping and drag/lift instabilities, and its application to dry inclined cable galloping." *Journal of Fluids and Structures*, 22(2), 229–252.

Macdonald, J. H. G., and Larose, G. L. (2008a). "Two-degree-of-freedom inclined cable galloping-Part 1: General formulation and solution for perfectly tuned system." *Journal of Wind Engineering and Industrial Aerodynamics*, 96(3), 291–307.

Macdonald, J. H. G., and Larose, G. L. (2008b). "Two-degree-of-freedom inclined cable galloping-Part 2: Analysis and prevention for arbitrary frequency ratio." *Journal of Wind Engineering and Industrial Aerodynamics*, 96(3), 308–326.

Main, J. A., and Jones, N. P. (2002). "Free vibrations of taut cable with attached damper. I: Linear viscous damper." *Journal Of Engineering Mechanics-Asce*, 128(10), 1062–1071.

Nguyen, C. H., Freda, A., Solari, G., and Tubino, F. (2015). "Aeroelastic instability and wind-excited response of complex lighting poles and antenna masts." *Engineering Structures*, Elsevier Ltd, 85, 264–276.

Nielsen, S. R. K., and Krenk, S. (2003). "Whirling motion of a shallow cable with viscous dampers." *Journal of Sound and Vibration*, 265(2), 417–435.

Nikitas, N., and Macdonald, J. H. G. (2014). "Misconceptions and generalisations of the Den Hartog galloping criterion." *Journal of Engineering Mechanics, ASCE*, 140(4), 1–11.

Pacheco, B. M., Fujino, Y., and Sulekh, A. (1993). "Estimation Curve for Modal Damping in Stay Cables with Viscous Damper." *Journal of Structural Engineering*, 119(6), 1961–1979.

Piccardo, G. (1993). "A methodology for the study of coupled aeroelastic phenomena." *Journal of Wind Engineering and Industrial Aerodynamics*, 48(2–3), 241–252.

Richardson, A. S. (1988). "Predicting Galloping Amplitudes." *Journal of Engineering Mechanics, ASCE*, 114(4), 716–273.

Uno, K., Kitagawa, S., Tsutsumi, H., Inoue, A., and Nakaya, S. (1991). "A Simple Method of Designing Cable Vibration Dampers of Cable-stayed Bridges." *JSCE Journal of*

Structural Engineering, 37A, 789–798.

Veletsos, A. S., and Ventura, C. E. (1986). “Modal analysis of non-classically damped linear systems.” *Earthquake Engineering and Structural Dynamics*, 14(January 1985), 217–243.

Yoneda, M., and Maeda, K. (1989). “A study on practical estimation method for structural damping of stay cable with damper.” *Proceedings of the Canada–Japan Workshop on Bridge Aerodynamics*, 119–128.

Yu, B. P., Desai, Y. M., Shah, A. H., and Popplewelp, N. (1993a). “Three-degree-of-freedom model for galloping. Part I: formulation.” *Journal of Engineering Mechanics, ASCE*, 119(12), 2404–2425.

Yu, B. P., Desai, Y. M., Shah, A. H., and Popplewelp, N. (1993b). “Three-degree-of-freedom model for galloping. Part II: solutions.” *Journal of Engineering Mechanics, ASCE*, 119(12), 2426–2448.

List of figure captions

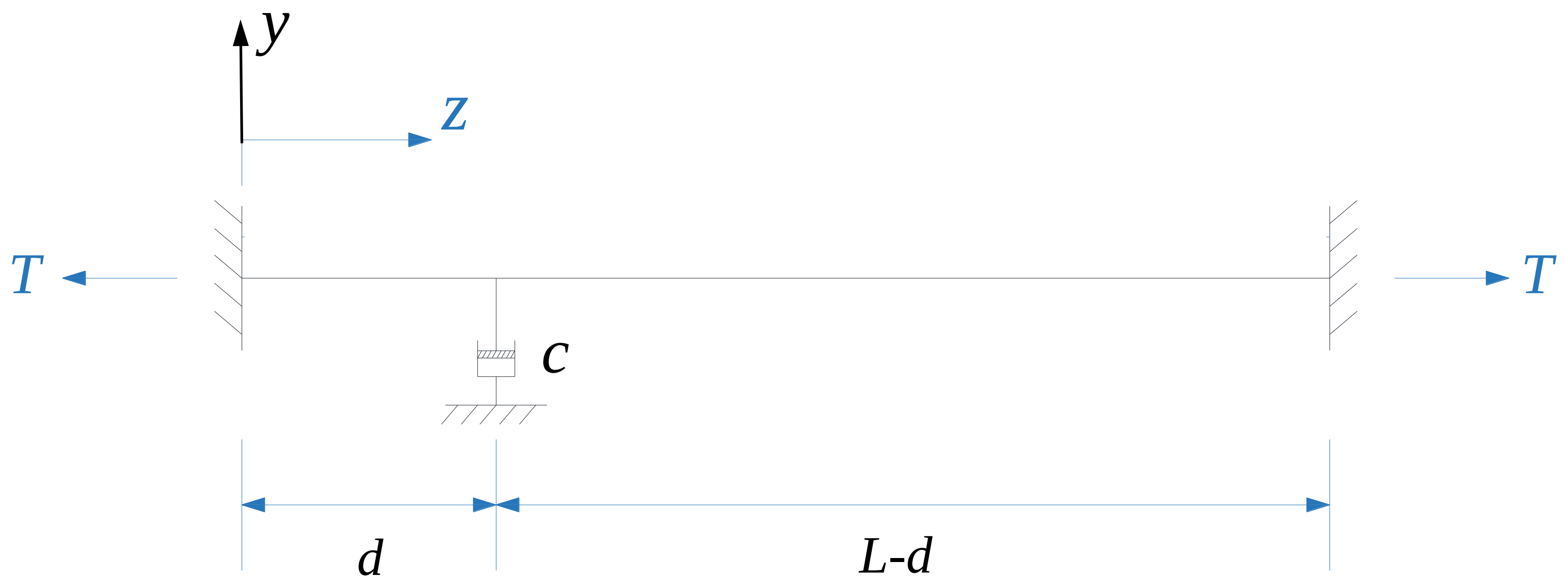

y
z
T
T
c
d
L-d

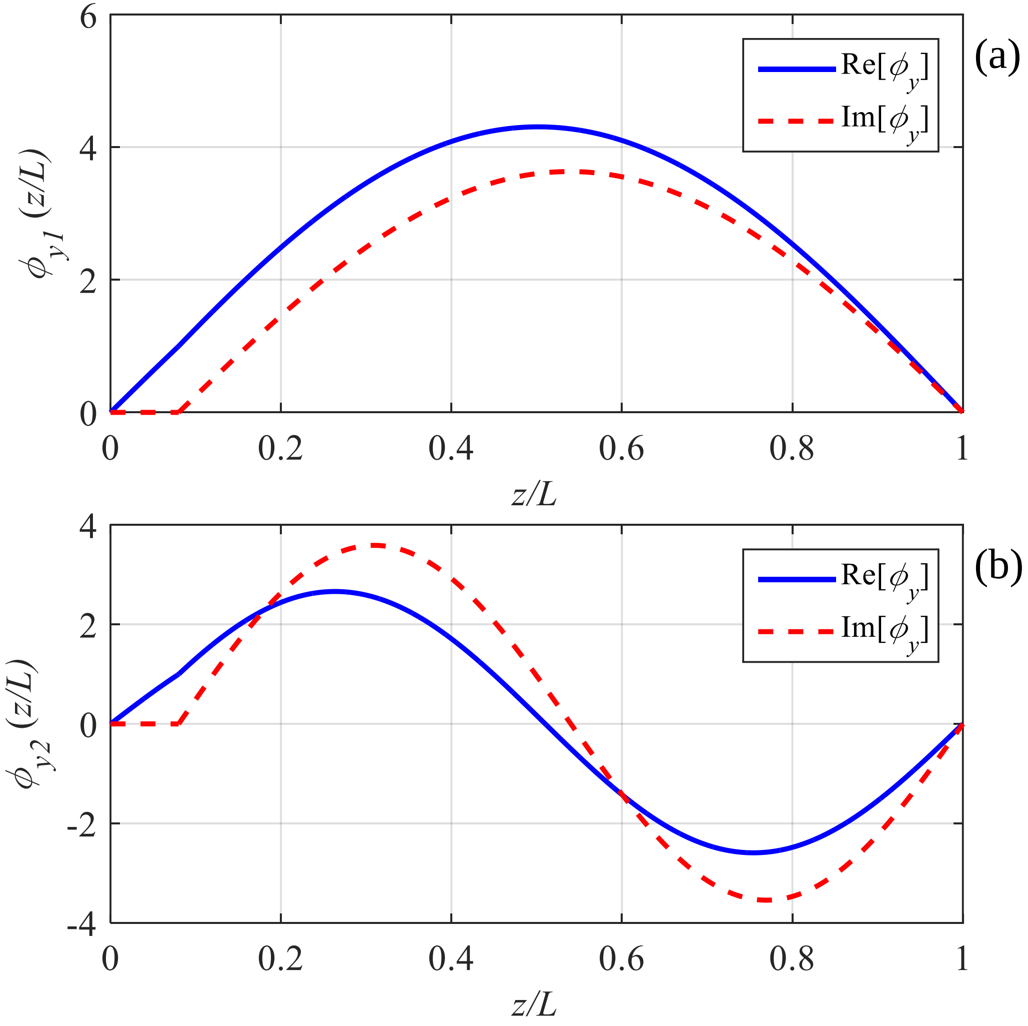

(a)
Re[ϕ_y]
Im[ϕ_y]
ϕ_{y1} (z/L)
z/L
0
0.2
0.4
0.6
0.8
1
6
4
2
0
(b)
Re[ϕ_y]
Im[ϕ_y]
ϕ_{y2} (z/L)
z/L
4
2
0
-2
-4

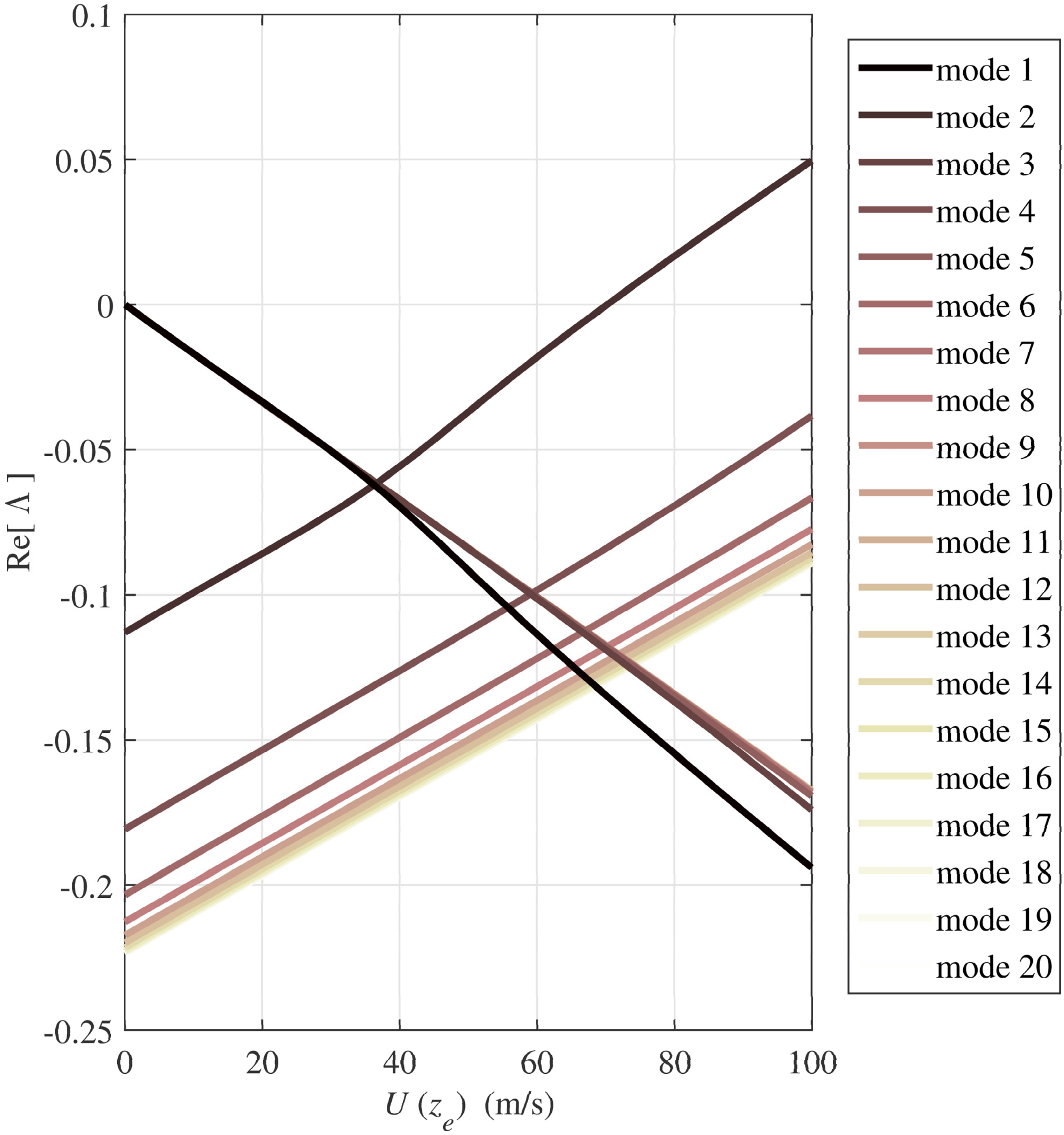
0.1
0.05
0
-0.05
-0.1
-0.15
-0.2
-0.25
Re[Λ]
0
20
40
60
80
100
U (z_e) (m/s)
mode 1
mode 2
mode 3
mode 4
mode 5
mode 6
mode 7
mode 8
mode 9
mode 10
mode 11
mode 12
mode 13
mode 14
mode 15
mode 16
mode 17
mode 18
mode 19
mode 20

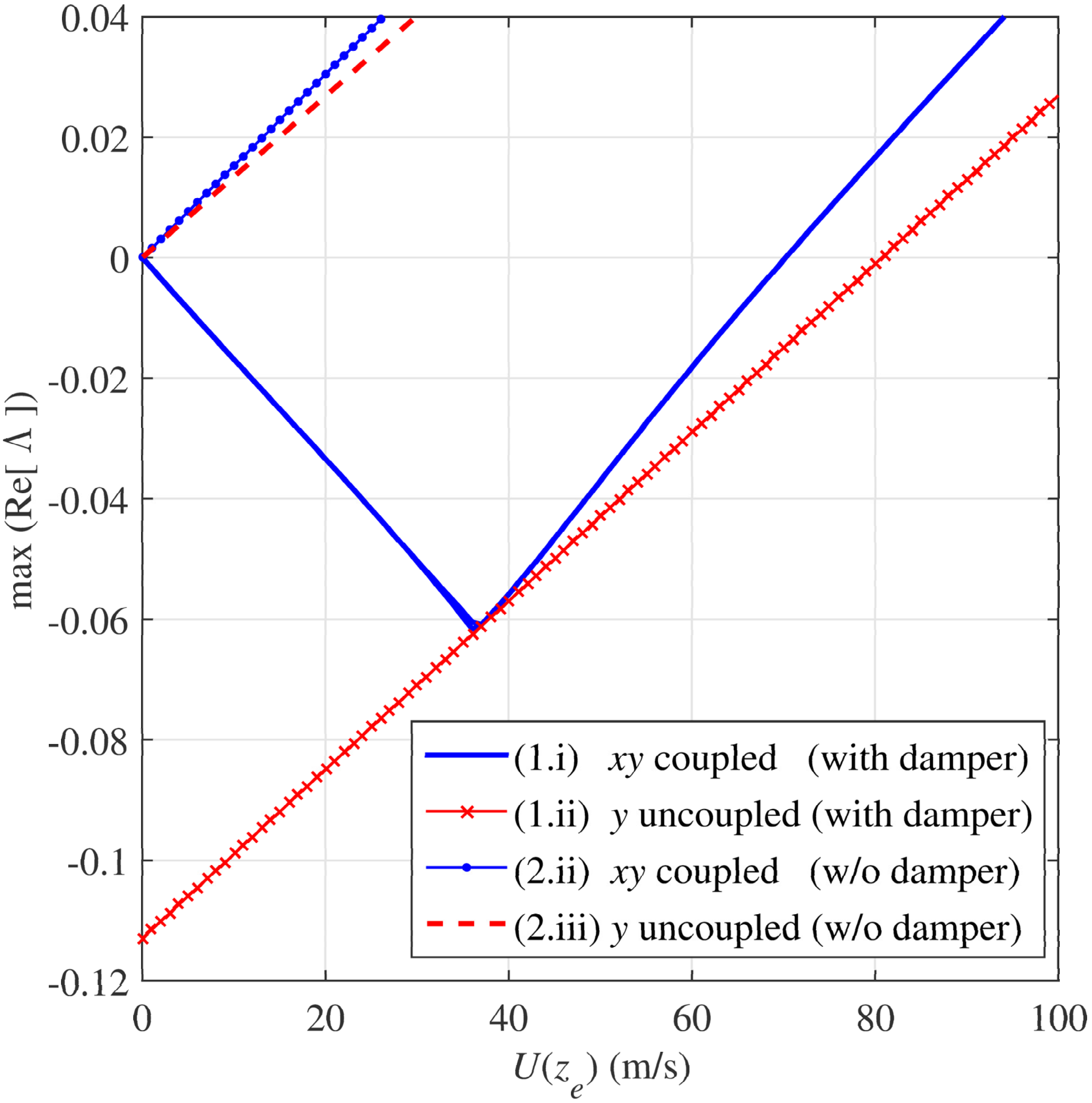

0.04
0.02
0
-0.02
-0.04
-0.06
-0.08
-0.1
-0.12
max (Re[Λ])
0
20
40
60
80
100
U(z_e) (m/s)
(1.i) xy coupled (with damper)
(1.ii) y uncoupled (with damper)
(2.ii) xy coupled (w/o damper)
(2.iii) y uncoupled (w/o damper)

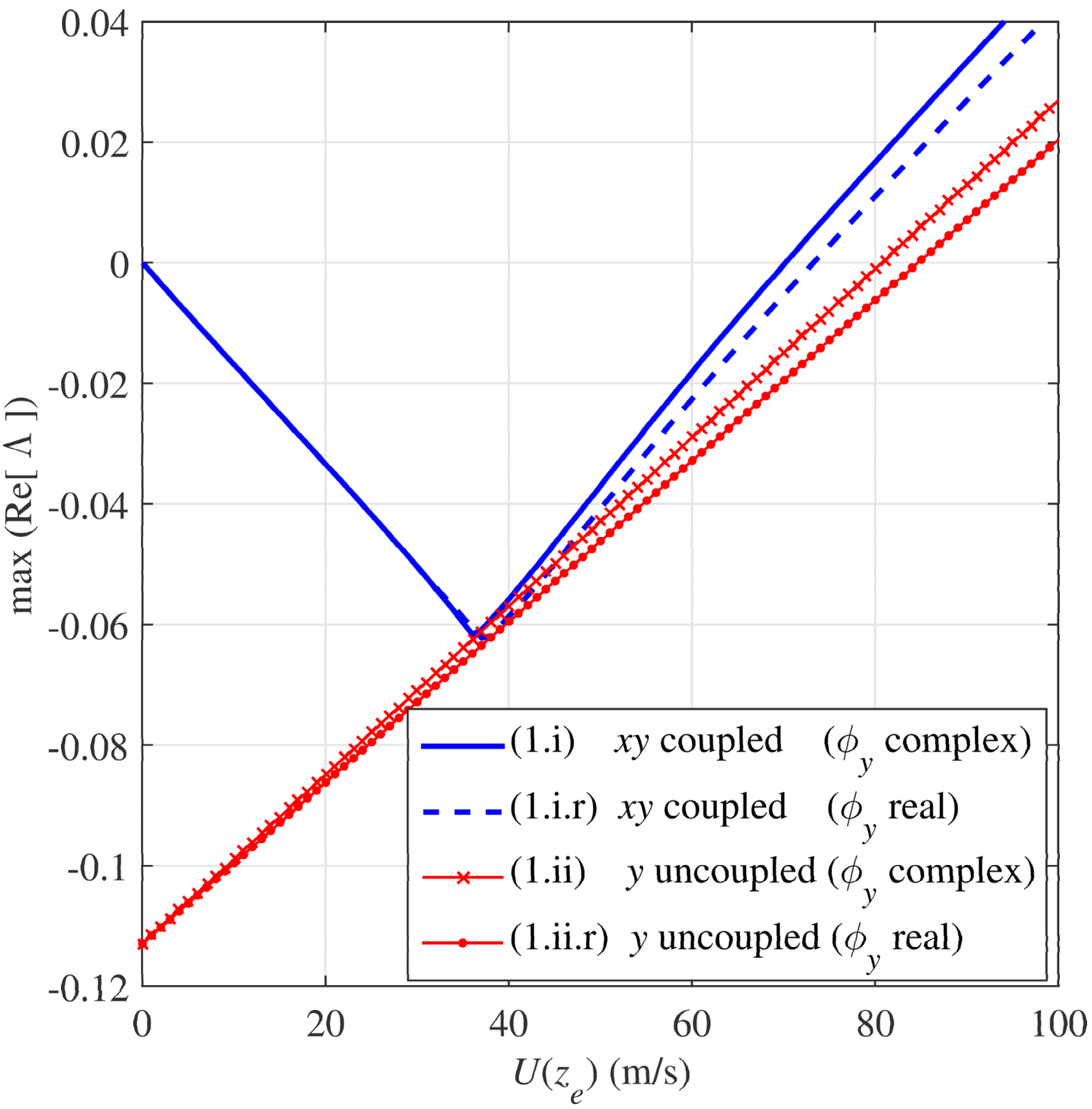

0.04
0.02
0
-0.02
-0.04
-0.06
-0.08
-0.1
-0.12
max (Re[Λ])
0
20
40
60
80
100
U(z_e) (m/s)
(1.i) xy coupled (ϕ_y complex)
(1.i.r) xy coupled (ϕ_y real)
(1.ii) y uncoupled (ϕ_y complex)
(1.ii.r) y uncoupled (ϕ_y real)